FAILURE PROBABILITY OF FLOOD DEFENCE STRUCTURES/ SYSTEMS IN RISK ANALYSIS FOR EXTREME STORM SURGES

Marie Naulin[1], Andreas Kortenhaus[1] and Hocine Oumeraci[1]

Extreme storm surges can cause failures of flood defences resulting in severe flooding of the hinterland and catastrophic damages. In order to quantify the risk of flooding, an integrated risk analysis is being performed within the German 'XtremRisK' project wherein one subproject failure probabilities of flood defences are determined. In this paper, the failure probability calculations of flood defence structures and systems under the loading of extreme storm surges are discussed. Moreover, the analysis of dike breaches and breach development is briefly introduced. Preliminary results of the failure probabilities and the breach modelling are presented using the example of the estuarine urban area of Hamburg, Germany. These results are put in context of an integrated risk analysis approach for extreme storm surges.

Keywords: failure probability, failure mechanisms, risk analysis, flood defences, storm surge, breaching

INTRODUCTION

In the past, storm surges have led to major damages, also along the German coastline. Due to climate change and sea level rise it may be expected that coasts will be exposed to increasing risks in the coming decades (IPCC 2007). In order to enhance the knowledge in extreme storm surge predictions, the assessment of the related risk and possible counter measures, the German joint research project XtremRisK was initiated (Oumeraci et al. 2009). The general aim of the project is to quantify the overall flood risk under present and future climate change conditions for an open coast (Island of Sylt, North Sea) and an estuarine urban area (Hamburg, Germany). For this purpose, an integrated risk analysis approach according to the source-pathway-receptor model (Fig. 1) is applied. The source-pathway-receptor concept has already been used in flood risk analysis and systematically addresses (Oumeraci 2004):

- The sources of the risk (storm surge)
- The risk pathways (way the risk "travels", e.g. along coastal defences or other storm surge protection measures)
- The receptors of risk which can be assets (houses, industry, farming area, etc.) or people

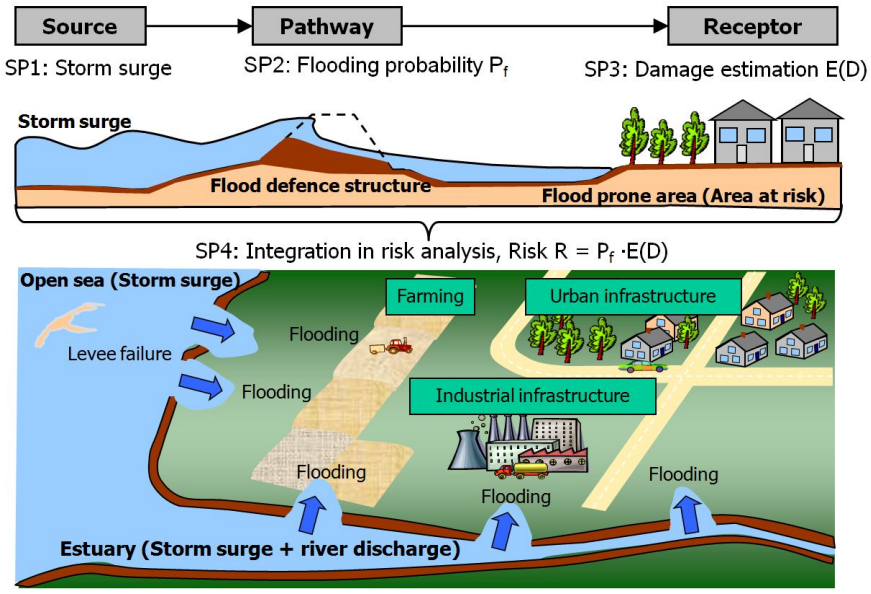

Figure 1. Source-pathway-receptor concept and associated subprojects (SP) in XtremRisK (Oumeraci et al. 2009).

[1] Department of Hydromechanics and Coastal Engineering, Leichtweiß-Institute for Hydraulic Engineering and Water Resources (LWI), Technische Universität Braunschweig, Beethovenstr. 51a, D-38106 Braunschweig, Germany, hyku@tu-braunschweig.de

The overall approach of XtremRisK comprises four subprojects which deal with risk sources, risk pathways, risk receptors, and their integration as follows (Fig. 1):

- Subproject 1 - Extreme storm surges (Risk sources)
- Subproject 2 - Loading, failure, breaching and breach development of flood defence structures (Risk pathways)
- Subproject 3 - Damage assessment and evaluation (Risk receptors)
- Subproject 4 - Risk analysis, risk evaluation and recommendations for risk mitigation (Integration)

Flood risk is defined as the product of flooding probability P_f and related consequences E(D). Hence, one of the key tasks is to predict the first component of the flood risk, i.e. the failure probability of the flood protection systems which is assumed equivalent to the probability of the hinterland being flooded. Within subproject 2 of XtremRisK, the failure probabilities of coastal flood defences used in these case studies are determined. Moreover, initial flooding conditions at the breaching locations (breach width, breach hydrograph, etc.) will be determined. The overall results will be delivered to subproject 3 of XtremRisK for inundation modelling and to subproject 4 for risk integration.

This paper presents the research work of subproject 2. First, the pilot sites, Hamburg and Sylt Island, are introduced. Second, the applied methodology of subproject 2 is presented. For this purpose, an overview including the main objectives is given. Furthermore, the methods of the reliability analysis are described. This includes an analysis of the failure mechanisms and fault trees and an introduction of the applied software tools. Moreover, the methods for breach modelling are briefly introduced. Third, preliminary results of the failure probabilities and the breach modelling using the example of one subarea of the pilot site in Hamburg are presented. These results are put in context of an integrated risk analysis approach used in XtremRisK and illustrate how they may contribute to risk mitigation in these areas. Finally, a summary is given, including a brief description of future prospects.

PILOT SITES

The pilot sites, Hamburg and Sylt Island, are located in the northern part of Germany (Fig. 2). The city of Hamburg is located in the Estuary of the Elbe River and has been chosen as an example for an estuarine urban area. As an example for an open coast, the island of Sylt in the North Sea is analysed.

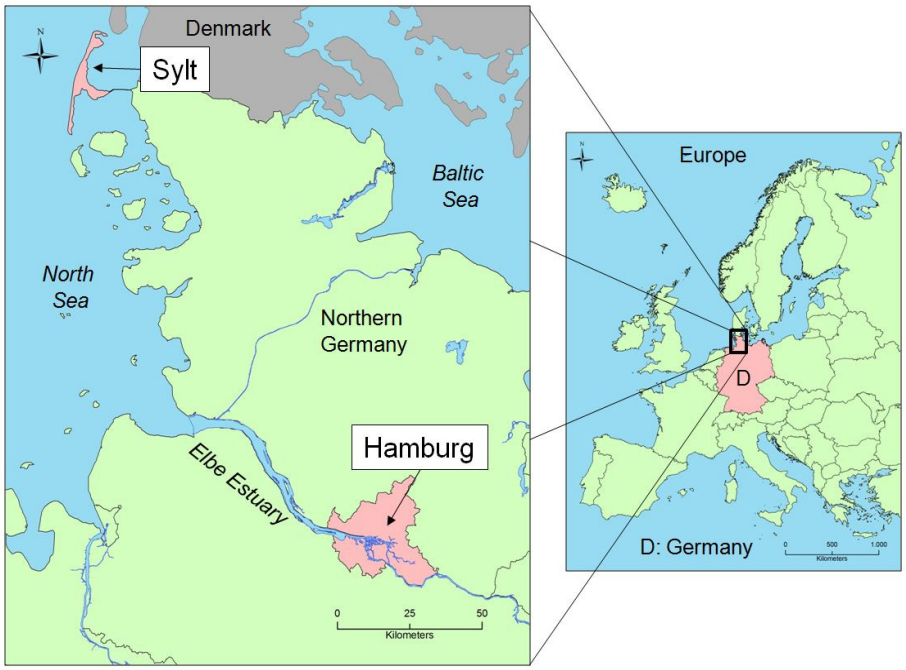

Figure 2. Location of pilot sites selected for this study: Hamburg and Sylt Island.

Hamburg is a mega-city with 1.8 million inhabitants and represents the second largest city of Germany. The city is as a centre for trade, transportation and services one of the most important industrial sites in Germany, e.g. the port is one of the world's leading seaports.

Hamburg's flood defence structures consist mainly of flood defence walls and dikes with sand core, clay layer and grass cover. Moreover, a great variety of structures to close the openings of the flood defence line is found such as flood defence gates, tidal gates, flood barriers, etc.

In contrast, the Island of Sylt has about 21,000 inhabitants whereof half of the residents live in the city of Westerland. However, Sylt is frequently used as tourist area. In 2009 almost 900,000 guests with approx. 7.0 million guest-nights were counted. Besides residential area, nature reserves and agricultural land can be found on the island.

On the east side of Sylt Island the same types of flood defences as in Hamburg are found while the west side of the Island is mainly protected by natural dunes which are annually supported by beach nourishments.

The main hydraulic conditions of the pilot sites for Hamburg and Sylt Island are summarised in Tab. 1. In the past, both pilot sites have suffered severe damages caused by extreme storm surges. In Hamburg the 1962 storm surge led to several dike breaches where more than 300 people lost their lives. At Sylt, due to the thin shape of the island, the risk of a full barrier breach exists. Until now breaches of foredunes could be observed at storm surges in 1962, 1981 and 1982.

Table 1. Main hydraulic characteristics of the pilot sites.

	Hamburg	Sylt Island
Mean high tide:	~ 2.1 mNN	~ 1.0 mNN
Highest storm surge:	6.45 mNN (1976)	4.05 mNN (1981)
Design water level	7.30 mNN	4.50 mNN
Max. waves:	H_S ~ 0.6 m, T_p ~ 4 s	H_S ~ 5.0 m, T_p ~ 14 s
Mean river discharge:	708 m³/s	-
Highest river discharge:	3,620 m³/s (1940)	-

mNN = datum for water level in Germany

Since an analysis of the total area of the pilot sites, Hamburg and Sylt, would exceed the work capacity in the framework of XtremRisK, typical subareas with characteristic properties were selected (Fig. 3). In Hamburg the subareas of Wilhelmsburg, Polder Hamburg Süd, and a part of the centre of the city were selected for the detailed study (Fig. 3a). At Sylt Island the subareas of Westerland and Hörnum were selected (Fig. 3b). Due to the typical properties of the subareas, the developed methods can be easily transferred to other coastal or estuarine areas.

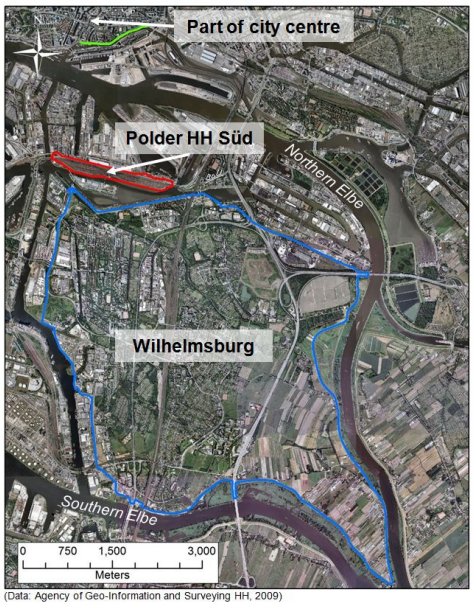

(a) Subareas of Hamburg.

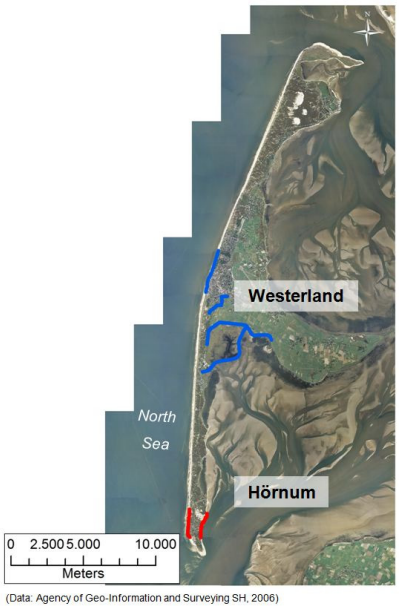

(b) Subareas of Sylt Island.

Figure 3. Maps of selected subareas and associated flood defence lines of the pilot sites Hamburg and Sylt.

METHODOLOGY OF SUBPROJECT 2 IN XTREMRISK

Overview

Within subproject 2 (SP 2) the loading and stability of coastal defences under extreme storm surges are analysed. For this purpose a reliability analysis is performed in order to calculate the failure probabilities of the coastal flood defences. Moreover, in case of structural failure of sea dikes or coastal dunes the breaching of these defences is analysed in order to describe the initial conditions of the flood wave at the breach for an inundation modelling of the hinterland.

These main tasks and results of SP 2 are summarised in a flow chart in Fig. 4. As input for the analysis, the water and wave parameters of an extreme storm surge event with its occurrence probability are provided by SP 1. Within SP 2 an analysis of the flood defence line is carried out in order to subdivide the flood defence line into characteristic sections and in order to determine the input parameters of the characteristic properties of the flood defences such as type of structure, geometric and geotechnical parameters as well as hydraulic conditions such as water depth and wave conditions.

On this basis, a reliability analysis and breach modelling is performed. For the reliability analysis, the uncertainties of model and input parameters are considered as well as different failure mechanisms described by associated limit state equations are analysed using a fault tree approach. The results of the probability of flooding are delivered to SP 4 for risk integration.

Moreover, the fault tree analysis allows determining the probability of breaching of flood defences such as dunes and dikes and gives an indication of the causes of the breach initiation, e.g. wave impact on the outer slope or overtopping on the inner slope. Based on these results for the identified sections (with a high probability of breaching), breach initiation and breach development are analysed using different breach models. The results of the initial condition of the flood wave (breach outflow hydrograph, breach width etc.) are delivered to SP 3 where an inundation modelling of the hinterland and a damage estimation are performed.

The applied methods within SP 2, i.e. the analysis of the flood defence line of the pilot sites, the reliability analysis and the breach modelling, will be introduced in more detail in the following sections.

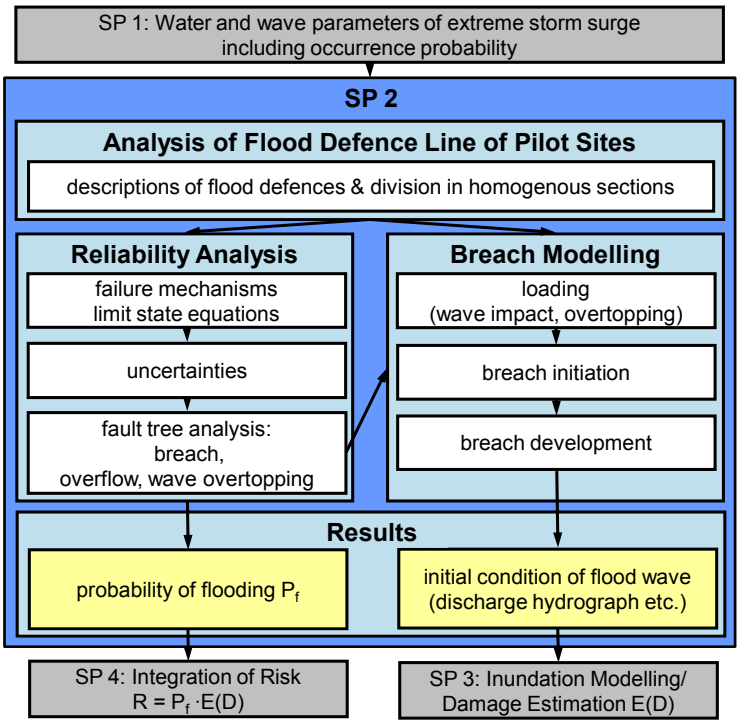

Figure 4. Flow chart of subproject 2 of XtremRisK and links to other subprojects (SP).

Analysis of Flood Defence Line

Input parameters describing the characteristics of the flood defences are needed in order to perform reliability analysis and breach modelling. As stated before, characteristic subareas of pilot sites for Sylt and Hamburg were selected. For these subareas, an overview and a detailed parameterisation of all flood defence structures were performed based on an intensive data collection in collaboration with the local flood defence authorities of Hamburg and Sylt. Therefore, inventory data and data from the measurements of the coastal defences as well as geological surveys and digital elevation models were analysed. The data preparation was mostly performed in a geographical information system (GIS).

The flood defence line of each subarea was then divided in sections with similar characteristics such as type of structure, geometric and geotechnical parameters. Moreover, the hydraulic conditions such as water level and wave conditions were considered for the subdivision. It is assumed that these segments are homogenous. For these sections, all input parameters and their uncertainties are investigated based on the results of the intensive data collection and analysis.

Reliability Analysis

Using a probabilistic approach by taking into account the uncertainties of both input parameters and models, a reliability analysis for flood defences is carried out. Therefore, the conditional failure probabilities are calculated for different extreme storm surge scenarios. The procedure of calculating conditional failure probabilities for different extreme storm surge scenarios is chosen since this offers the possibility to perform an event-based inundation modelling and damage estimation.

The extreme storm surge scenarios under current and future climate change conditions include wave parameters and water levels as well as an occurrence probability determined by SP 1 of XtremRisK. For more information it is referred to the following section where preliminary results are introduced.

Within the reliability analysis the loading (S) and the resistance (R) representing the strength of all components of the flood defence systems are determined. For this purpose, different failure modes described by limit state equations are analysed using a fault tree approach which will be described in the following subsections.

Failure Mechanism Since the flood defence line consists of a number of different types of flood defence structures, all failure mechanisms of the documented flood defence structures are examined. In reliability theory a failure mode is expressed by comparing the strength R and loading S by means of process models in a limit state equation (LSE):

$$Z = R - S \tag{1}$$

R expresses the strength of the flood defence structure and can be a function of geometric or geotechnical parameters of the structure such as e.g. crest level, thickness of the revetment blocks or cohesion of the soil. S represents the loading and can for example be a function of the hydraulic loading conditions driven by water level, wave action, groundwater etc. The structure fails if the loading exceeds the strength, i.e. $S > R$, and the structure is safe for $S \leq R$.

Exemplarily one failure mechanism is shown in Fig. 5. The non-structural failure mechanism overflow is expressed by a limit state equation comparing the actual energy height of water overflowing the flood defence with the admissible energy height of water calculated from critical discharge.

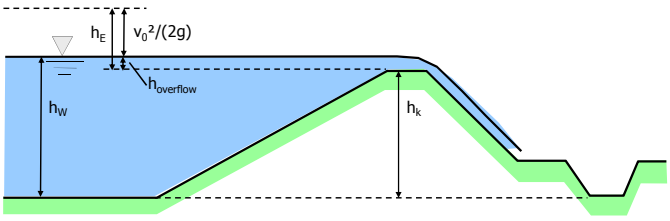

$$z = h_{E,adm} - h_E$$

h_E = actual energy height of water overflowing the flood defence [m]
$h_{E,adm}$ = admissible energy height of water calculated from critical overflow discharge [m]

Figure 5. Example failure mechanism overflow with limit state equation (definition sketch).

The different failure mechanisms are analysed and reviewed based on the results of previous projects such as FLOODsite (Allsop et al. 2007) and ProDeich (Kortenhaus 2003). In general there are over 80 different limit state equations available in order to describe the failure mechanisms of the different flood defences. For all flood defence types non-structural failure such as overflow and wave overtopping is considered. Moreover, failure modes leading to a structural failure, e.g. breaching of dikes, are considered.

On this basis, relevant failure mechanisms are selected for the existing types of flood defences under consideration of the loading of extreme storm surges. Moreover, knowledge gaps are identified and an attempt is made to close them, e.g. by updating or developing missing limit state equations.

Fault Tree Analysis For each of the structure types the failure mechanisms are organised in a fault tree. The structure of the fault tree represents the different chains of events leading to an overall failure of the flood defence structure (top event) which is defined in this study as flooding of the hinterland. An overview of a general structure of a fault tree is presented in Fig. 6. It shows a generic fault tree combining different limit state equations for dikes. As it can be seen, not only structural failure leading to a breach of the dike but also non-structural failure as overflow and wave-overtopping are considered in the fault tree. A more detailed extract of a fault tree for dikes is presented in the following section where preliminary results are discussed.

The existing fault trees are also reviewed based on a literature study. The knowledge gaps are identified and attempted to close, e.g. by including new or updated limit state equations and developing missing fault trees for structures not yet considered.

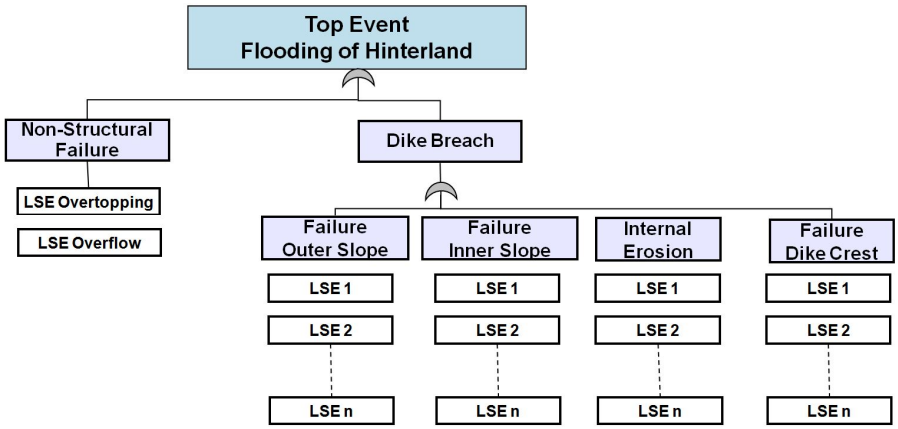

Figure 6. General structure of fault tree for dikes combining different limit state equations (LSE).

Failure Probability Calculations The failure probability is calculated by applying Monte-Carlo-Simulations. The calculations of failure probabilities will be first carried out for each failure mechanism. These results of all failure modes are combined using a fault tree analysis which leads to the failure probability of the top event of the fault tree, i.e. flooding probability of the hinterland for each flood defence section. From this, the overall failure probability for the flood defence system for each subarea is calculated using again a fault tree approach.

For the failure probability calculations software tools such as FLOODsite software tool RELIABLE (Van Gelder et al. 2008) or ProDeich (Kortenhaus 2003) are applied. For this purpose, all relevant failure mechanisms and fault trees are implemented within the software tools.

Preliminary results of the failure probability calculations are presented in the next section. However, first the methodology of the breach modelling is introduced in the following subsection.

Breach Modelling

The total failure of the flood defences includes breach and breach development of flood defence structures such as sea dikes and natural barriers such as dunes. In case of breaching the process is further analysed and modelled in order to specify the initial conditions of the flood wave for the inundation modelling of the hinterland. For this purpose, the results of the reliability analysis indicate if and where breaching might occur, i.e. sections with a high probability of breaching. Moreover, the identification of causes and failure modes that may induce an initial breach can be assessed by a fault tree analysis.

The causes of breach initiation depend on the structure of the dike and on the hydraulic and morphological boundary conditions. In general, several causes for the initiation and formation of a breach can be distinguished, e.g. wave overtopping, overflow, wave impact and seepage (Fig. 7).

Within the breach modelling the following main failure mechanisms which may lead to the breaching of sea dikes are considered (TAW 1999):

- Erosion and sliding initiated on landside slope by wave overtopping and overflow
- Erosion of seaward slope resulting from breaking wave impacts and the flow induced by wave run-up and run-down

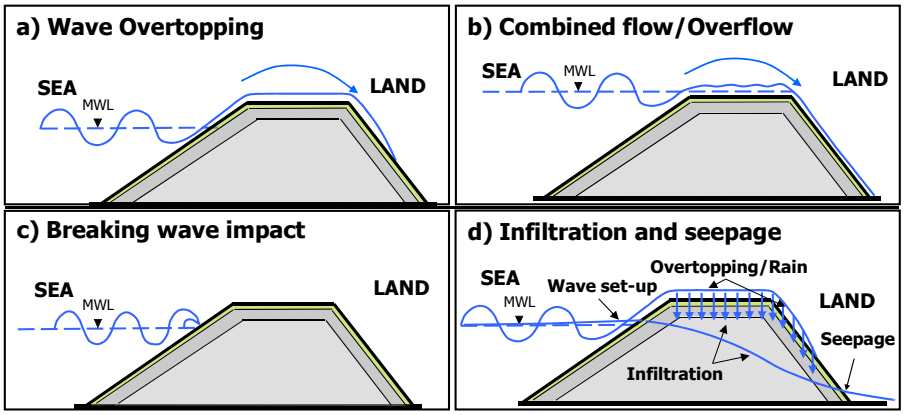

Figure 7. Causes of breach initiation (D'Eliso 2007).

The main differences in the processes of breaching initiated on the seaside and on the landside of a dike can be attributed to the loading conditions and the characteristic of the erosion processes. The loading on the seaside slope (breaking wave impact) acts on a very limited area and during very short, intermittent periods, while the shear stress related to wave overtopping acts on the entire landside slope and during longer time periods.

Depending on the causes of breach initiation there are different breaching models available, e.g.:

- Breaching initiated on the landside by wave overtopping and overflow:
  D'Eliso et al. (2006), D'Eliso (2007), Tuan & Oumeraci (2010b)
- Breaching initiated on the seaside by breaking wave impacts:
  Stanczak et al. (2008), Stanczak (2008)

Depending on the loading conditions (wave overtopping/ overflow or breaking wave impacts) and thus depending on the breach initiation (landside or seaside) one of the above introduced breaching models is applied to the case study area.

As a result, the breach development can be described in time with specifications on breach initiation, breach duration, and the final breach width and depth. Furthermore, the outflow hydrograph of the breach can be estimated. These results will be used as input parameters for the simulation of the flood wave propagation and inundation of the hinterland and the related damages in the study areas.

PRELIMINARY RESULTS

Preliminary results are exemplarily given for the dikes of the subarea of the Elbe Island Wilhelmsburg in Hamburg (Fig. 8). In the following section, the hydraulic conditions of an extreme storm surge event as well as the results of the analysis of the flood defence line, the reliability analysis and the breach modelling are exemplarily described.

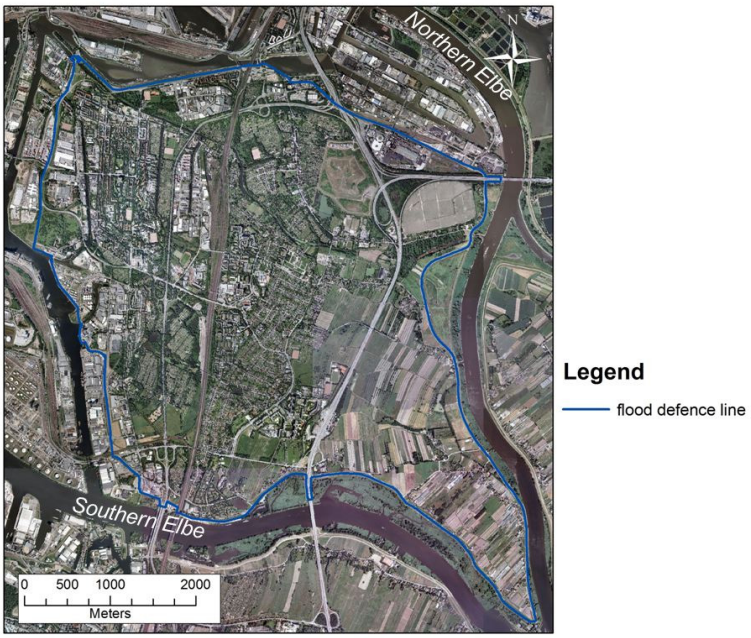

Figure 8. Map of the study subarea Wilhelmsburg, Hamburg.

Hydraulic Conditions

Input parameters of the hydraulic conditions of an extreme storm surge under current climate conditions calculated by SP 1 of XtremRisK were used. The storm surge event has a peak water level of 8.0 mNN which is 5.9 m above the mean high tide and 0.7 m above the design water level of Wilhelmsburg. The occurrence probability was determined to $1.0 \cdot 10^{-5}$ per year (Wahl et al. 2010). The wave conditions were estimated considering the highest possible on-site wave conditions, i.e. a significant wave height of $H_S = 0.55$ m with a peak period of $T_p = 4.0$ s.

For the reliability analysis, the duration of the peak water level was estimated to 6.0 hours. Hence, the preliminary results of the failure probabilities represent an overestimation of what might actually occur. However, for the breach modelling the unsteady conditions in terms of the time series of the water level were considered.

Analysis of Flood Defence Line

In Wilhelmsburg, Hamburg, the main part of the flood defence line, i.e. 19 km out of 23 km, consists of dikes. The remaining part of the flood defence line includes flood defence walls. Moreover, there are structures to close the openings of the flood defence line such as flood defence gates, tidal gates, flood barriers, etc.

The dikes are built with a sand core, clay layer and grass cover (Fig. 9). The crown heights of the dikes vary from 7.80 mNN to 8.35 mNN and in general the outer and inner slopes are 1/3.

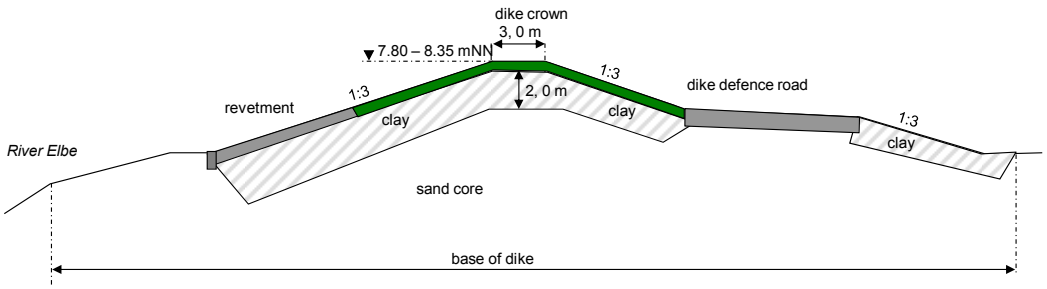

Figure 9. Typical cross section of dikes in Wilhelmsburg, Hamburg.

The result of the subdivision of Wilhelmsburg flood defence line into "homogenous" sections according to similar characteristics such as type of structure, geometric and geotechnical parameters is shown in Fig. 10. Overall the flood defence line is divided into 84 sections. Out of these sections a total number of 62 segments are dikes and 7 sections are walls. Furthermore, there are 15 so called "point structures" such as gates etc.

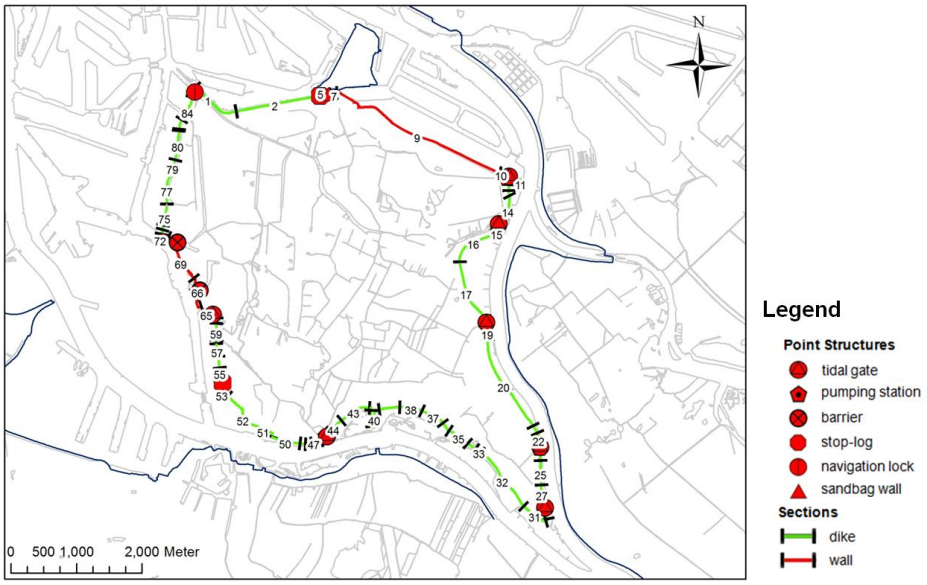

Figure 10. Sections of the flood defence line of the study subarea Wilhelmsburg, Hamburg.

Failure Probabilities

For the reliability analysis a total of 22 failure mechanisms are considered. Two failure modes leading to non-structural failure, i.e. overflow and wave overtopping, as well as 20 failure mechanisms inducing dike breaching are analysed.

The combination of all failure modes leading to the top event of inundation is performed by a fault tree approach whereas the general structure of the fault tree shown in Fig. 6 is applied. Considering the uncertainties of input and model parameters, the failure probability calculations were carried out by using Monte-Carlo-Simulations.

As results, the conditional failure probabilities of the storm surge event with a peak water level of 8.0 mNN and an occurrence probability of $1.0 \cdot 10^{-5}$ per year were calculated for each of the 62 dike sections. The results of the failure probabilities are exemplarily shown in Fig. 11 for the first dike section in Wilhelmsburg, Hamburg. The overall result of the failure probabilities of the top event, i.e. flooding of the hinterland, reaches the highest possible value of $P_f = 1.0$ per year.

The dominating failure mechanism leading to the high probability of flooding is identified as non-structural failure in terms of wave overtopping ($P_f = 1.0$). Moreover, the probability of overflow is also high with a value of $P_f = 0.8$ per year.

The limit state equations for these failure modes compare the admissible overtopping discharge with the actual overtopping discharge. It is noticed that the analysed peak water level of the storm surge is in some parts higher than the heights of the dike crowns. Moreover, the admissible discharge is easily exceeded since the admissible value is set to a rather low rate of 0.5 l/s/m by the local authority for public flood defences of Hamburg.

As a next step, the structural stability is analysed, i.e. it is examined if the dikes are resistant enough to hydraulic loading of the extreme storm surge event. Therefore, the results of the failure probabilities of the failure mechanisms leading to a dike breach are examined. As shown in Fig. 11 the probability of a dike breach of this section is $7.5 \cdot 10^{-2}$ per year resulting from a failure of the inner slope. The results in the fault tree illustrate that the hydraulic boundary conditions for the critical velocity on the inner slope are fulfilled which leads to a probability of $7.5 \cdot 10^{-2}$ per year for an erosion of the inner slope.

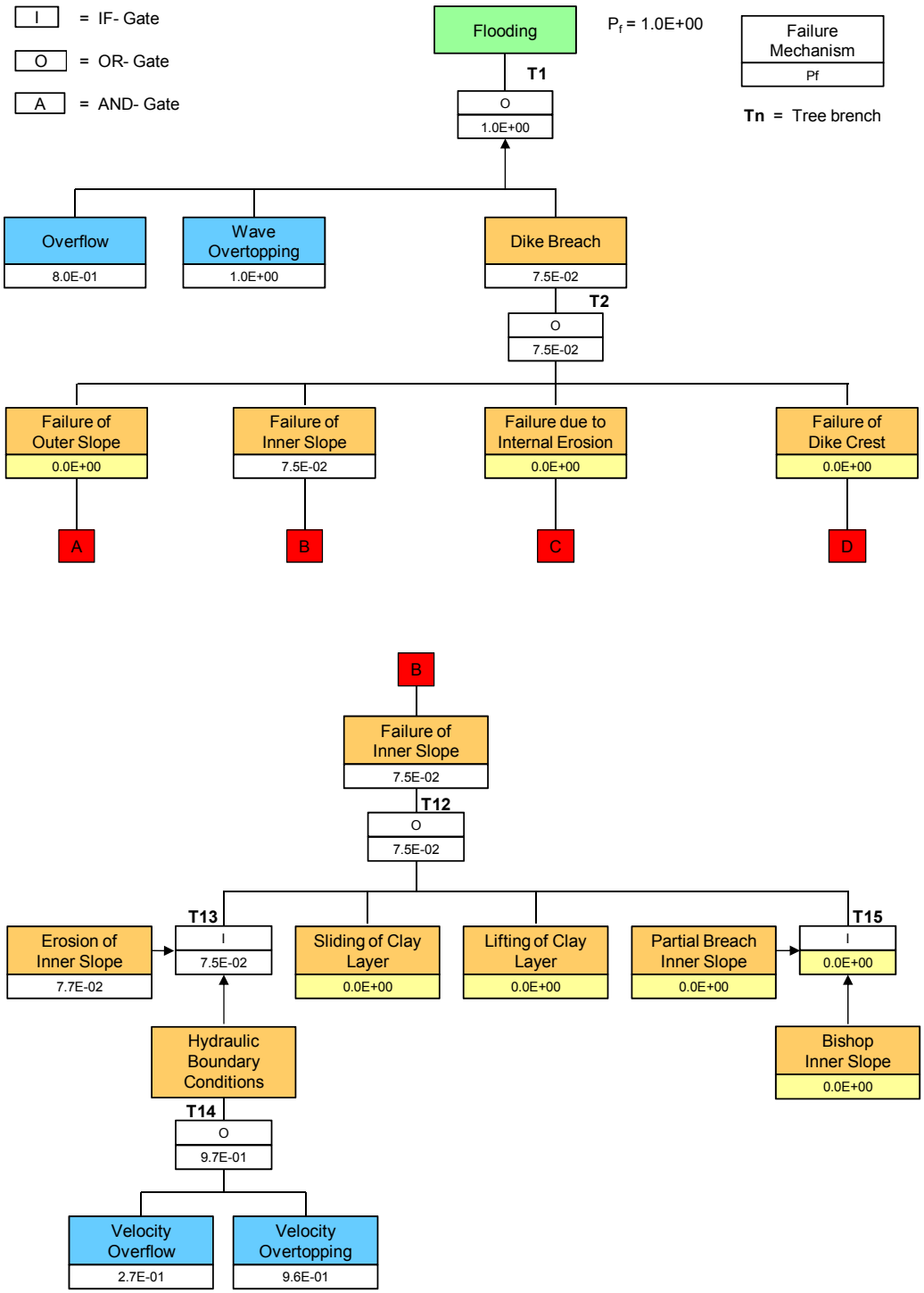

Figure 11. Failure probabilities and extract of fault tree for the first dike section in Wilhelmsburg, Hamburg.

The failure probability calculations were carried out for all 62 dike segments. As shown in Fig. 12, the overall results of the failure probabilities of the top event, i.e. flooding of the hinterland, reach very high values of almost $P_f = 1.0$ per year for all dike sections of the flood defence line. The dominating failure mechanisms leading to the high probability of flooding are identified as non-structural failure in terms of wave overtopping and overflow.

In order to analyse the structural stability of the inner slope, the results of the failure probabilities of the failure of the inner dike slope are examined. As shown in Fig. 13 for most dikes the failure probabilities of the failure of the inner dike slope are rather low ($1.0 \cdot 10^{-4}$ per year). Only in some areas higher values (between $1.0 \cdot 10^{-2}$ and $1.0 \cdot 10^{-3}$ per year) are calculated. These dike sections are identified as weak spots since they have less resistant inner slopes or are exposed to more severe hydraulic loading.

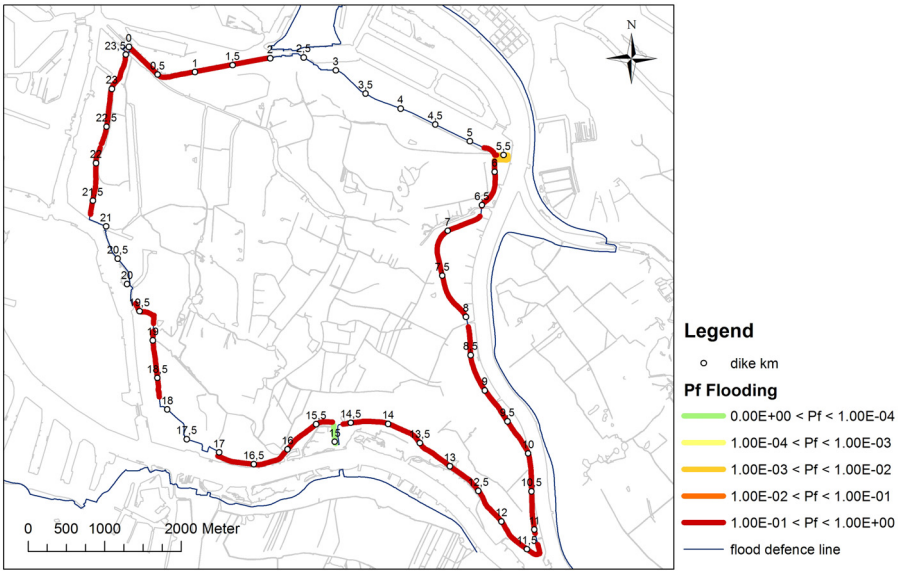

Figure 12. Failure probabilities of the top event, i.e. flooding of the hinterland.

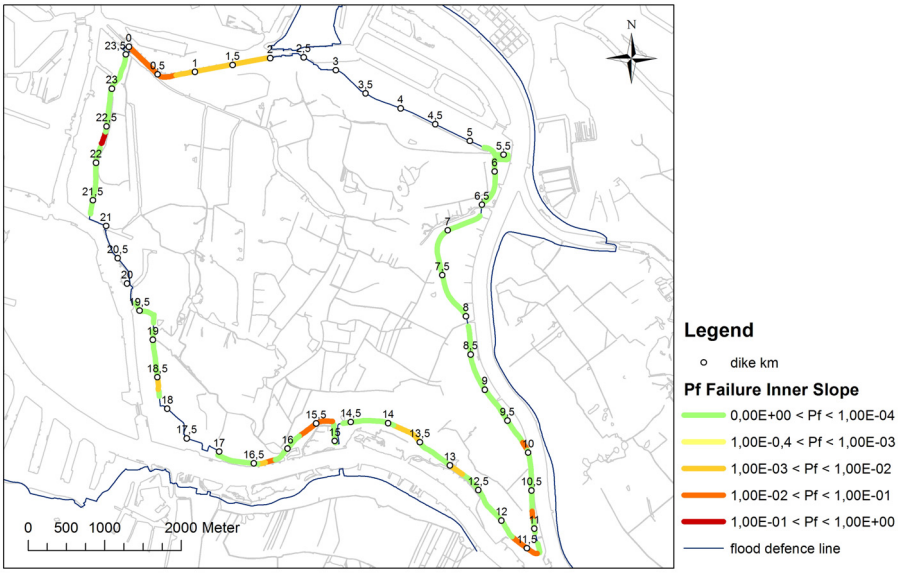

Figure 13. Failure probabilities of the failure of the inner dike slope.

Modelling of Breaching

The results of the fault tree analysis revealed that overflow and wave overtopping represent the major forcing. For this reason the BREID model simulating wave overtopping-induced erosion of the inner slope of grassed sea-dikes is applied to the case study area of Hamburg Wilhelmsburg. The BREID model is a numerical model for simulating BREaching of Inhomogeneous sea Dikes (BREID) developed by Tuan & Oumeraci (2010a,b). The model consists of three different modules: fixed-bed overtopping, breach initiation and breach development.

The hydrodynamic module for the numerical simulation of wave overtopping on sea dikes is based on the nonlinear shallow water equations. The model can be extended with an additional source term related to the roller energy dissipation in the depth-averaged momentum equation to account for the additional effect of the surface roller motion breaking waves (Tuan & Oumeraci 2010a).

The modelling of breach initiation is based on the approach of excess bed shear for grass erosion. For the determination of the bed shear stress, the flow structure of wave overtopping on the inner slope is refined according to turbulent wall jet formulations in order to account for the high turbulence with entrained air bubbles for the conditions of wave overtopping on grass slopes. The critical velocity for grass erosion is determined based on depth-dependent strength concept together with the mobilized shear strength coefficient from Eq. 2 (Tuan & Oumeraci 2010b):

$$u_{gs,c} = 0.64 \log\left(\frac{8.8h}{d_a}\right)\sqrt{\Delta g d_a + \frac{1}{\rho}\left(0.6\,C_f + \mu_r C_r^w\right)} \qquad (2)$$

With $u_{gs,c}$ = critical velocity of grass slopes [m/s]; h = flow depth [m], d_a = (0.003 ~ 0.005 m) size of the clay detaching aggregates [m]; $\Delta = ((\rho s - \rho)/\rho)$ relative density of clay [-]; ρ_s = saturated clay density [kg/m³]; g = gravitational gravity [m/s²]; ρ = water density [kg/m³]; C_f=(0.035c) fatigue rupture strength of clay [kN/m²]; c = clay cohesion [kN/m²], μ_r = (Cr/Crw < 1) root mobilized strength coefficient [-]; C_r = root cohesion [kN/m²]; C_r^w = root cohesion estimated according to Wu et al. (1979) [kN/m²]

The dike section no. 1 in Wilhelmsburg, Hamburg, has a higher probability of failure of the inner slope (Fig. 13). Therefore, the breach initiation of this dike profile is analysed. The main input parameters for the simulation such as hydraulic conditions, dike geometry as wellas grass and clay properties are summarised in Tab. 2.

Table 2. Main input parameters for simulating grass erosion.

Parameter	Unit	Value
Hydraulics		
wave height H_{m0} at dike toe	m	0.55
peak period T_p	s	4.0
peak surge level (series above 7 mNN)	mNN	8.01
storm duration	hrs	3.16
Chezy coefficient: grass slope	$m^{0.5}/s$	30
inland water level	m	dry bed
Dike geometry		
crest level	m	7.88
dike slopes: inner (outer)	-	1/3 (1/3)
dike crest width B_c	m	2.78
grass thickness	m	0.20
clay cover thickness: inner, top, outer	m	1.30; 2.00; 1.50
Grass and clay properties		
clay cohesion c	kN/m^2	24
mean root tensile strength $t_{r,m}$	10^3 kN/m^2	20.5
reference RAR_0 (at depth 2.5 cm)	%	0.065
root decay parameter β	-	0.12
mobilized strength coefficient μ_r	-	0.60
grass erosion coefficient M_{gs}	$kg/m^2/s$	5.0E-03
clay erosion coefficient M_{gc}	$kg/m^2/s$	5.0E-03

Wave Overtopping As results of simulating overtopping, the mean overtopping discharge q_{bmean} [m³/s/m] and the associated depth-averaged overtopping flow velocities u_b [m/s] for a dike profile are obtained. The results of the discharges and flow velocities at the dike crown and at the end of the dike slope are exemplarily shown in Fig. 14.

As seen in Fig. 14a, significant wave overtopping and overflow with discharges higher than 0.5 l/s/m comprises a period of 2.76 hours (from t = 827 s until t = 10,768 s). Within this period a total water volume of ca. 1152 m³/m overtops the dike. Hence, the computed average discharge equals 0.12 m³/s/m. At the dike crown the computed maximum discharge equals 1.36 m³/s/m.

Considering the results of several selected locations along the inner slope of the dike, the maximum depth-average velocity u_{max} with 5.33 m/s (Fig. 14b) was computed at the end of the inner dike slope while the layer thickness equals 0.14 m.

The main results of the computed fixed-bed overtopping are summarised in Tab. 3.

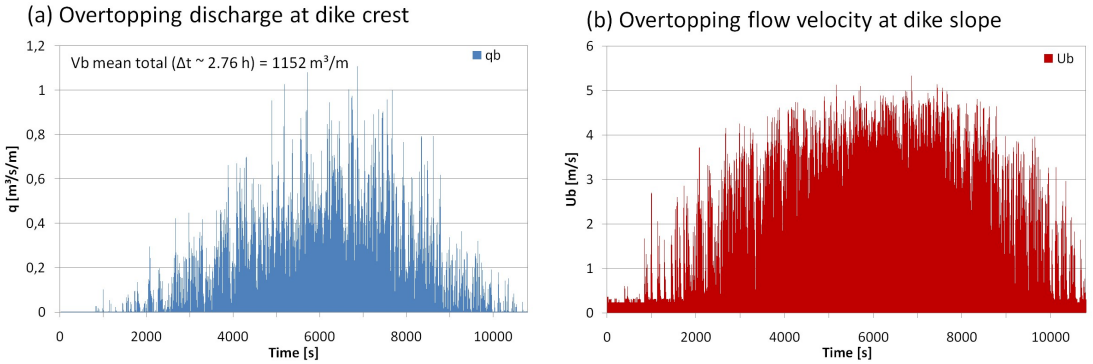

Figure 14. Mean overtopping discharge for time interval Δt=1s (q_b) at dike crone and depth-averaged flow velocity (u_b) at the dike slope.

Table 3. Main results of computed overtopping.

Parameter	Unit	Value
average discharge q (Δt = 2.76 hrs)	m³/s/m	0.12
maximum discharge q	m³/s/m	1.69
total overtopping volume V (Δt = 2.76 hrs)	m³/m	1152
maximum depth-average velocity on slope u_{max}	m/s	5.33

Breach Initiation To simulate grass erosion, the input parameters as addressed in Tab. 2 were applied. The numerical modelling of wave overtopping-induced erosion of grassed inner sea-dike slopes is based on the approach of excess bed shear for grass erosion. In general, the same parameters as for the simulation of fixed-bed overtopping are computed for a dike profile per one meter width. Besides the discharges, the water layer thickness and the flow velocity, for the mobile bed data also the height of the dike profile considering the reduction due to erosion are available.

The critical velocities for grass $u_{gs,c}$ resulting from Eq. (2) with an average overtopping thickness h_b = 0.04 m are 4.6 m/s and 3.5 m/s for the top surface and for a depth of 5.0 cm, respectively. Also from Eq. (2), the critical velocity $u_{s,c}$ for the bare clay is 0.86 m/s, which is significantly smaller than those for the grass reinforced clays.

The results of the simulation of grass erosion initiated by the computed overtopping are shown in Fig. 15. The maximal height reduction (in z plane) is only 7.0 cm. Hence, the grass erosion is initiated but the erosion of the clay cover has not started yet.

The low erosion rate can be explained by looking at the critical velocity for grass. Eq. (2) emphasises that the critical velocity of grass depends on the flow depth. With a decrease of the overtopping thickness the critical velocity decreases and vice versa. To give an example, for h_b =0.01 m and h_b =0.23 m the critical velocity of grass $u_{gs,c}$ at the surface is 3.2 m/s and 6.5 m/s, respectively. It seems as if for this simulation high velocities are reached at the same time as the flow depths increase (during overflow conditions). Therefore, in these times of flow depth with h_b = 0.20 m the critical velocity of grass is higher and is not exceeded by the actual velocity.

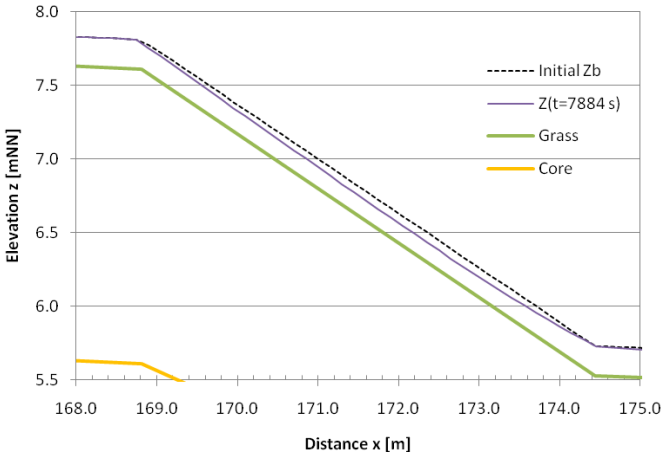

Figure 15. Grass erosion initiated by computed overtopping.

As a next step, it is intended to analyse the effects of possible weak spots, e.g. holes or cracks in the grass layer. Furthermore, after the breach initiation the breach development will be analysed. As results of the modelling the breach width and the breach outflow hydrograph will be obtained in order to specify the initial conditions of the flood wave at the breach for inundation modelling of the hinterland.

SUMMARY AND FUTURE PROSPECTS

The overall aim of XtremRisK which consists of four subprojects is to perform an integrated flood risk analysis for extreme storm surge scenarios for an estuarine urban area using the example of the city of Hamburg and for an open coast using the example of the island of Sylt. In this paper the focus is put on subproject 2 which deals with loading, failure and breaching of coastal flood defence structures.

In more detail, within subproject 2 the failure probabilities are determined and the breaching of coastal flood defences is analysed. Investigating failure probabilities of flood defences represents a first step in order to quantify the risk of coastal flooding. Moreover, the results of the analysis of possible breaches of sea dikes or dunes allow to determine the initial conditions of the flood wave at the breach for inundation modelling.

In this paper, the methods to determine failure probabilities of flood defence structures as well as the methods for breaching modelling of dikes or dunes are outlined. Furthermore, preliminary results of failure probability calculations and breach modelling are given exemplarily for a ring dike in Hamburg. It is shown how the reliability analysis allows identifying relevant failure mechanisms and "weaker" dike sections with a higher probability of flooding. For an extreme storm surge scenario with an occurrence probability of $1.0 \cdot 10^{-5}$ per year most of the dike sections considered here will either overflow or overtop (failure probability of $P_f = 1.0$).

Since wave overtopping and overflow were identified as the major forcing in this scenario, a breach model simulating overtopping and grass erosion on the inner slope was applied (Tuan & Oumeraci, 2010a,b). A dike section with a failure probability of $7.5 \cdot 10^{-2}$ per year for an erosion of the inner slope was selected for the modelling. The mean overtopping discharge which overtops or overflows the dike was determined to 0.12 m³/s/m over a period of 2.76 hours. Hence, the extreme storm surge event directly leads to severe flooding. Moreover, the results of the breach initiation modelling showed that the erosion of the grass layer was initiated to a depth of only 7.0 cm; i.e. a breach would not develop. Further studies will analyse the effects of possible weak spots in the grass layer such as holes or cracks.

The overall results of flooding probabilities and initial flooding conditions will be delivered to subproject 3 in order to model the inundation for damage estimation and to subproject 4 in order to integrate the results in an integrated risk analysis (Burzel et al. 2010).

Future prospects within subproject 2 include further applications of the introduced methods of reliability analysis and of breach modelling for both pilot sites. Moreover, it is intended to update and further develop missing limit state equations and fault trees for failure mechanisms or structures not yet considered.

ACKNOWLEDGEMENTS

The project XtremRisK is funded by the German Federal Ministry of Education and Research BMBF (Project No. 03 F 0483 A). The funding is gratefully acknowledged by the authors.

Moreover, the financial support by the German Port Technology Association (HTG) for the conference participation of the first author is gratefully appreciated.

Furthermore, the collaboration and the provision of data by the Cooperative and Consulting Partners of the project such as LKN-SH, HPA and LSBG are also gratefully acknowledged.

REFERENCES

Allsop, N.W.H.; Buijs, F.; Morris, M.W.; Hassan, R.; Young, M.J.; Doorn, N.; Van der Meer, J.W.; Kortenhaus, A.; Van Gelder, P.H.A.J.M.; Dyer, M.; Redaelli, M.; Visser, P.J.; Bettess, R.; Lesniewska, D. (2007): Failure mechanisms for flood defence structures. FLOODsite - Integrated Flood Risk Assessment and Management Methodologies, T04-05-01, Task 4, 150 p.

Burzel, A.; Dassanayake, D.; Naulin, M.; Kortenhaus, A.; Oumeraci, H.; Wahl, T.; Mudersbach, C.; Jensen, J.; Gönnert, G.; Sossidi, K.; Ujeyl, G.; Pasche, E. (2010): Integrated flood risk analysis for extreme storm surges (XtremRisK), Proc. 32nd International Conference Coastal Engineering (ICCE), Shanghai, China.

D'Eliso, C. (2007): Breaching of sea dikes initiated by wave overtopping. A tiered and modular modelling approach. Ph.D. thesis, Dissertation, Civil Engineering Faculty, Leichtweiß-Institut für Wasserbau, Technische Universität Braunschweig, University of Florence, 142 p.

D'Eliso, C.; Oumeraci, H.; Kortenhaus, A. (2006): Breaching of coastal dikes induced by wave overtopping. Proc. 30th International Conference Coastal Engineering (ICCE), San Diego, USA, ASCE, vol. 3, pp. 2844-2856.

IPCC (2007): Climate change 2007: WG II: Impacts, Adaptation and Vulnerability, Chap. 6. Coastal systems and low lying areas. Intergovernmental Panel on Climate Change (IPCC), Cambridge.

Kortenhaus, A. (2003): Probabilistische Methoden für Nordseedeiche. Ph.D. thesis, Dissertation, Fachbereich Bauingenieurwesen, Leichtweiß-Institut für Wasserbau, Technische Universität Braunschweig (22.01.2003), Braunschweig, Germany, 154 p.

Oumeraci, H. (2004): Sustainable coastal flood defences: scientific and modelling challenges towards an integrated risk-based design concept. Proc. First IMA International Conference on Flood Risk Assessment, IMA - Institute of Mathematics and its Applications, Session 1, Bath, UK, pp. 9-24.

Oumeraci, H.; Jensen, J.; Gönnert, G.; Pasche, E.; Kortenhaus, A.; Naulin, M.; Wahl, T.; Thumm, S.; Ujeyl, G.; Gershovich, I.; Burzel, A. (2009): Flood risk analysis for a megacity: The German XtremRisK project, Proc. Conference on Road Map towards a Flood Resilient Urban Environment, Paris France, 8 p.

Stanczak, G. (2008): Breaching of sea dikes initiated from the seaside by breaking wave impacts. Ph.D. thesis, Dissertation, Civil Engineering Faculty, Leichtweiß-Institut für Wasserbau, Technische Universität Braunschweig, University of Florence, 143 p..

Stanczak, G., Oumeraci, H.; Kortenhaus, A. (2008): Detailed computational model for the breaching of sea dikes initiated by breaking wave impacts. Proc. 31st International Conference Coastal Engineering (ICCE). Hamburg, Germany, vol. 2, pp. 1787-1799.

Tuan, T.Q.; Oumeraci, H. (2010a): A numerical model of wave overtopping on seadikes. Coastal Engineering, vol. 57, pp. 757-772.

Tuan, T.Q.; Oumeraci, H. (2010b): Numerical modelling of wave overtopping-induced erosion of grassed inner sea-dike slopes. Coastal Engineering, submitted.

TAW (1999): Water retaining earth structures. Technische Adviescommissie voor de Waterkeringen (TAW), Technical report, Delft, The Netherlands, 105 p.

Van Gelder, P.H.A.J.M.; Buijs, F.; Van, C.M.; ter Horst, W.L.A.; Kanning, W.; Nejad, M.; Gupta, S.; Shams, R.; Van Erp, N.; Gouldby, B.; Kingston, G.; Sayers, P.B.; Wills, M.; Kortenhaus, A.; Lambrecht, H.-J. (2008): Reliability analysis of flood sea defence structures and systems. FLOODsite Executive Summary T07-09-20, 21 p.

Wahl, T.; Jensen, J.; Mudersbach, C. (2010): A Multivariate Statistical Model for Advanced Storm Surge Analyses in the North Sea, Proc. 32nd International Conference Coastal Engineering (ICCE), Shanghai, China.

Wu, T.H.; McKinel, W.P.I.; Swanston, D.N. (1979): Strength of tree roots and landslides on Prince of Wales Island, Alaska. Canadian Journal of Geotechnical Resources, 16, 1, pp. 19-33.